A pharmacophore modeling approach to design new taxol® mimics: towards the synthesis of potential anticancer and MDR-reversing agent

Michela L. Renzulli, Luc Rocheblave,[¥] Stanislava I. Avramova, Elena Galletti, Daniele Castagnolo, Laura Maccari,[§] Stefano Forli, Fabrizio Manetti, Federico Corelli, and Maurizio Botta*

Dipartimento Farmaco Chimico Tecnologico, Università degli Studi di Siena, via Aldo Moro, snc 53100 Siena, Italy

[¥]Laboratoire de Stéreochimie Dynamique et Chiralité, Faculté des Sciences de Saint Jérôme, avenue Escadrille Normandie Niemen, 13397 Marseille cedex 20, France

[§]Sienabiotech S.p.A. Drug Design and Information Technologies, Via Fiorentina 1, 53100 Siena, Italy

E-mail: botta@unisi.it

Abstract

The remarkable therapeutic importance of taxane diterpenoids as anticancer drugs and their challenging structural complexity have stimulated worldwide enormous efforts. Our group developed a theoretic quantitative model describing the relationship between structure and biological activity of microtubules-stabilizing anticancer agents (MSAAs) aimed at gaining an insight into the specific structural features required for the ligand-receptor binding. The model was demonstrated to be able to estimate/predict the microtubule-stabilising activity for a series of taxanes and provided further details about the influence of each pharmacophore point on the ligand binding affinity. Molecular modeling studies from our group revealed that modified Taxuspines U and X could adopt a conformation similar to the bioactive conformation of paclitaxel and can be well accommodated within the pseudoreceptor model. Following the suggestions coming from the model we rationally designed and synthesized new simplified taxuspine U analogues. In particular, we developed a new methodology for the synthesis of such compounds involving a macrocyclisation reaction *via* RCM in presence of different functional groups.

Keywords: Microtubules-stabilizing anticancer agents (MSAAs), taxane diterpenoids, Taxuspine U and X, minireceptor model, ring closing metathesis (RCM)

Introduction

The emergence of Paclitaxel (Taxol®)[1] as one of the most promising anticancer natural products[2,3] has stimulated worldwide interest in phytochemical studies of Taxus species. Paclitaxel (**1**) and its semisintetic analogue docetaxel (**2**, Taxotere®) (Figure 1 and Table 1) exhibit potent antitumor activity against different cancers which have not been effectively treated by existing antitumor drugs. This is due to their unique ability to inhibit microtubules depolymerisation process by promoting the polymerisation of tubulin α,β-heterodimers and stabilizing the resulting polymer. This mechanism of action differs from that of antimitotic drugs such as colchicines, podophyllotoxin and the Vinca alkaloids, which inhibit microtubule assembly. Microtubules formed in the presence of Taxol® are resistant to depolymerisation by Ca^{2+} ions.[3]

Results and Discussion

The identification of features responsible for enhancing binding to the receptor of interest has always attracted the interest of medicinal chemists. Experimental protein structures (i.e., from X-ray crystallography or NMR studies) are commonly used to investigate details of the receptor-ligand interaction mode, ligand affinity data, and, subsequently, to rationally design novel chemical structures with improved properties as potential lead compounds (the so called structure-based drug design). Also, QSAR studies are applied to derive quantitative models able to describe structure-activity relationships with a regression analyses which identifies pharmacophoric elements or descriptor variables upon which the biological activity depends. As a result, this modeling technique could be of help in guiding the improvement of ligand activity.

The availability of tubulin experimental structures has stimulated many studies about the binding mode of anticancer agents acting on that protein. An interesting model for the binding of **1** to β-tubulin was proposed by Snyder and coworkers.[4] In this work, a conformational search of **1** was performed and the identified conformers were fitted into the experimental structure of tubulin. The complexes were then subjected to a refinement through molecular dynamics calculations leading to a T-shaped conformation for bound inhibitor and rationalization of the SAR data for paclitaxel. However, a discussion, at the quantitative level, on the relationships between structure and activity of **1**, was not reported in the paper.

In order to find a theoretical quantitative model able to describe the relationships between the structure and biological activity of microtubule stabilizing agents belonging to the family of Taxanes, we performed some studies intended at developing a minireceptor model.[5] The aim of the study was to gain an insight into the specific structural features required for the binding into the receptor and to provide further details about the influence of each pharmacophore point onto the ligand binding affinity. Notably, such a model could be applied in the rational design of ligands showing improved affinity towards tubulin.

PrGen software was selected to develop our minireceptor model.[6] The main step in model development is represented by the ligand equilibration protocol, which permits to better refine disposition of the binding site residues around the ligands, in conjunction with a flexible fitting of the ligands themselves within the receptor. Moreover, a regression model is calculated which is able to estimate binding affinity values of compounds used to build the minireceptor-ligands assembly or predict affinity of molecules external to the training set. Indeed, the minireceptor model takes into account two important aspects of modeling studies: generation of a pharmacophore model for ligands and fitting of this pharmacophore in a binding site derived from the experimental coordinates of tubulin. Both the 3D QSAR and the fitting step are developed simultaneously avoiding the limitation of considering, in separate steps, the three-dimensional properties of the ligands or refinement of the protein.

Table 1. Structural and biological properties of taxanes (1-14) and epothilones (15, 16, 18- 21) used in this study

Compd	R_1	R_2	R_3	R_4	R_5	R_6	R_7	X	ΔG_{exp}[a]	ΔG_{calc}[a]	$\Delta\Delta G$[a]	K_{exp}[a]	K_{calc}[a]
1[b]	PhCOO	AcO	OH	=O	AcO	Ph	Ph		-6.46	-6.63	-0.16	$1.5\cdot10^{-5}$	$7.8\cdot10^{-6}$
2	H	AcO	OH	=O	AcO	Ph	Ph		-3.14	-4.44	-1.30	$4.5\cdot10^{-3}$	$3.1\cdot10^{-3}$
3	(pCF$_3$)PhCOO	AcO	OH	=O	AcO	Ph	Ph		-5.42	-6.45	-1.03	$9.0\cdot10^{-5}$	$5.1\cdot10^{-5}$
4	PhCOO	OH	OH	=O	AcO	Ph	Ph		-3.38	-3.40	-0.02	$3.0\cdot10^{-3}$	$2.0\cdot10^{-3}$
5[c]	PhCOO	AcO	$NH_2CH_2CO_2$	=O	$NH_2CH_2CO_2$	Ph	tBuO		-6.36	-4.47	1.89	$1.8\cdot10^{-5}$	$2.1\cdot10^{-5}$
6	PhCOO	AcO	OH	OH	AcO	Ph	Ph		-6.63	-7.28	-0.65	$1.1\cdot10^{-5}$	$2.3\cdot10^{-5}$
7[c]	PhCOO	AcO	OH	=O	H	Ph	Ph		-6.86	-6.34	0.51	$7.6\cdot10^{-6}$	$3.8\cdot10^{-6}$
8[c]	PhCOO	AcO	OH	=O	AcO	C_6H_{11}	Ph		-7.18	-5.57	1.61	$4.4\cdot10^{-6}$	$6.6\cdot10^{-6}$
9[d]	PhCOO	AcO	OH	=O	OH	Ph	tBuO		-6.90	-6.16	0.74	$7.1\cdot10^{-6}$	$2.8\cdot10^{-5}$
10									-3.14	-3.50	-0.35	$4.5\cdot10^{-3}$	$6.1\cdot10^{-3}$
11[c]									-5.66	-4.92	-0.73	$6.0\cdot10^{-5}$	$1.3\cdot10^{-4}$
12[c]									-4.81	-5.07	-0.26	$2.6\cdot10^{-4}$	$1.6\cdot10^{-4}$
13[c]	OH								-5.23	-5.38	-0.14	$1.2\cdot10^{-4}$	$9.7\cdot10^{-5}$
14	AcO								-4.22	-4.89	-0.67	$7.1\cdot10^{-4}$	$2.2\cdot10^{-4}$
15[c]	H							O	-6.50	-5.13	1.37	$1.4\cdot10^{-5}$	$1.5\cdot10^{-4}$
16	Me							O	-7.23	-5.81	1.42	$4.0\cdot10^{-6}$	$4.6\cdot10^{-5}$
17	Me							NH					
18									-6.17	-6.29	-0.12	$2.5\cdot10^{-5}$	$2.0\cdot10^{-5}$
19[c]	Me								-7.34	-7.36	-0.02	$3.3\cdot10^{-6}$	$3.2\cdot10^{-6}$
20									-6.24	-5.03	1.21	$2.2\cdot10^{-5}$	$1.8\cdot10^{-4}$
21									-5.91	-4.97	0.93	$3.9\cdot10^{-5}$	$1.9\cdot10^{-4}$

[a]ΔG_{exp}: experimental value (kcal/mol); ΔG_{calc}: calculated value (kcal/mol); $\Delta\Delta G$: difference between ΔG_{exp} and ΔG_{calc} (kcal/mol). K_{exp}: experimental value (M); K_{calc}: calculated value (M). K_{exp} values have been converted into ΔG_{exp} by application of the Gibbs-Helmhotz equation. [b]Paclitaxel or Taxol®. [c]Compounds used to generate the test set. All the other compounds with the exception of compound **17** belong to the training set. [d]Docetaxel or Taxotere®.

The starting point of this work was represented by the 3D structure of the α,β-tubulin dimer (3.7 Å resolution, 1TUB entry of the Brookhaven Protein Data Bank) obtained by electron crystallography of zinc-induced tubulin sheets.[7] The experimental structure clearly showed the location of paclitaxel binding site in the β subunit but lacked the resolution to exactly define the whole ligand conformation. As a consequence, not all the amino acid residues were well solved and paclitaxel was replaced by the X-ray structure of docetaxel.[8]

In order to provide a 3D QSAR model for taxanes binding into β-tubulin, a shell of amino acids, together with a training set of taxanes (compounds **1-11**, **13**, and **14**, Figure 1, Table 1) was submitted to the ligand equilibration protocol implemented in PrGen software.

Accordingly, a correlation-coupled receptor minimization was alternated to free ligand relaxation in an iterative fashion until a satisfactory correlation coefficient and a root mean square deviation of experimental and calculated binding energies were obtained.

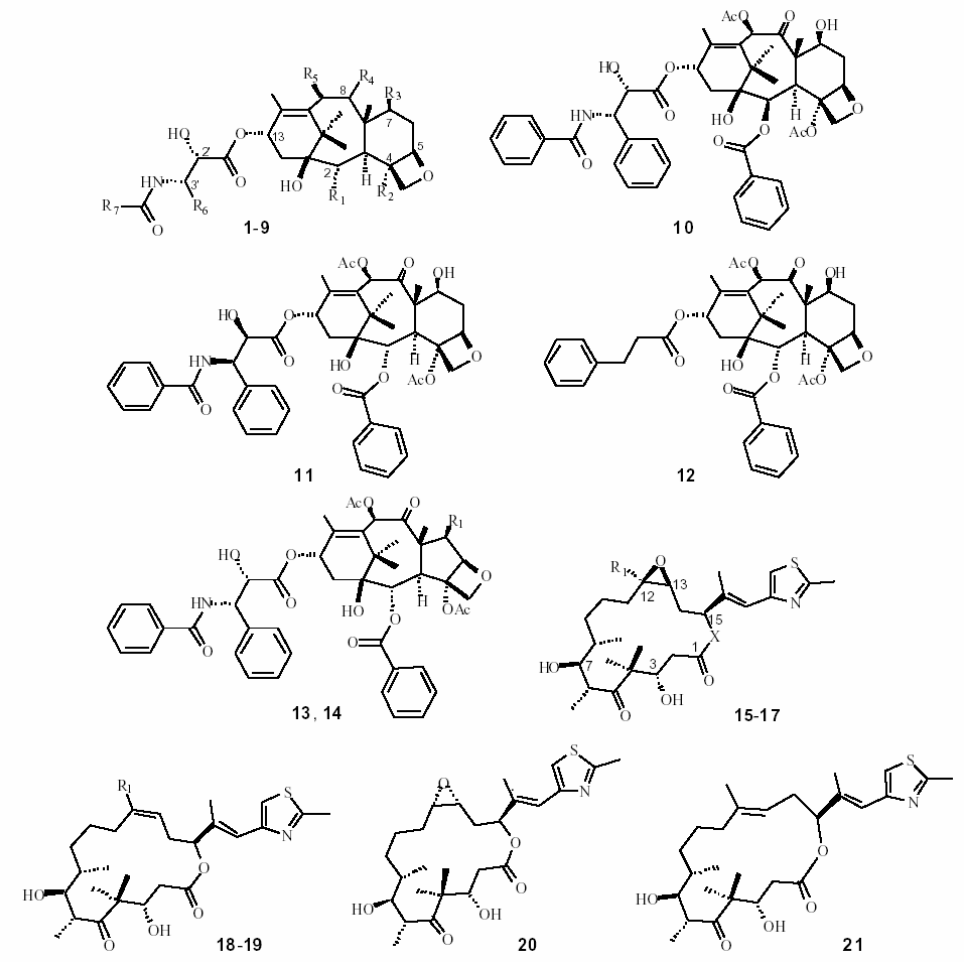

Figure 1

The resulting minireceptor, characterized by a correlation coefficient (R) of 0.97 and a root mean square deviation (rmsd) of 0.35 kcal/mol, was the first model providing, at a quantitative level, SARs between taxanes and tubulin binding site as derived from the experimental complex. The model identified the pharmacophore features of the ligands and the relative counterparts on the tubulin binding site, mainly interacting by hydrogen bonds and hydrophobic contacts. The binding site was represented by several hydrophobic pockets also establishing hydrogen bonds with taxanes (Fig. 1 and 2).

In detail, the C3' phenyl, C12 methyl, and C4 acetyl groups were located in a lipophilic region defined by Phe272, Leu230, Leu217, and Leu275, while the oxetane ring and C7 hydroxy group were at a close contact with a polar cluster of residues (Thr276, Ser277, and Arg278). Moreover, the northern side of the taxane macrocycle was fully accessible to the solvent, while His229 was interposed between the C3' benzamido and C2 benzoyl southern side chains. Hydrogen bonds involved the C7 hydroxy, C2 benzoyl, C3' amido, and C2' hydroxy group of ligands (Figure 2).

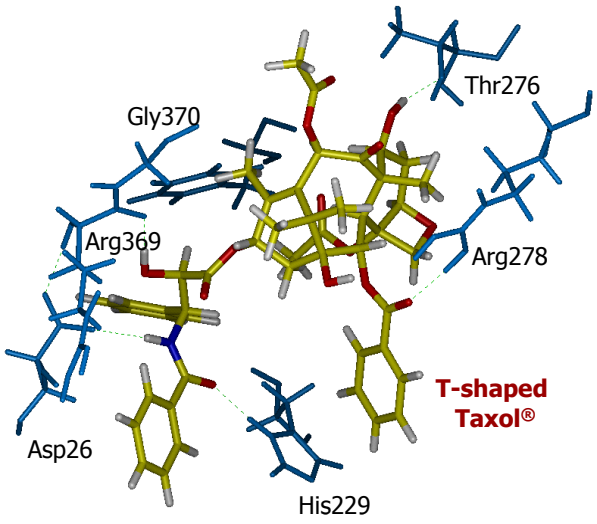

Figure 2. Paclitaxel (1) fitted into the minireceptor model for taxanes. Only the most important amino acid residues interacting with the ligand are shown.

The tubulin-ligands interactions found by the model were in perfect agreement with structure-activity relationship data collected from literature. Notably, modeled paclitaxel conformation resulting from the minireceptor approach closely resembled the recently proposed T-shaped one, which is supposed to be the bioactive conformation.[9]

The further point of this computational approach was represented by the fitting of epothilones (**15**, **16**, **18-21**, Figure 1 and Table 1) into the minireceptor model. At that time, no experimental structure of tubulin-epothilones complex was available. Thus, we have applied a two-step computational protocol aimed at generating a pharmacophoric hypothesis for both epothilones and taxanes (first step) to be translated into a minireceptor model of the tubulin

binding site, thus constituting a binding site inhibitors assembly. The latter, was used, to generate a regression model able to estimate or predict, at a quantitative level, biological data of the studied compounds (second step).[10]

The first step of this computational work was addressed by means of a ligand-based drug design (pharmacophore development) approach. For this purpose, we chose the refined structure of the α,β-tubulin at 3.5 Å resolution (1JFF entry in the Brookhaven Protein Data Bank).[11] Paclitaxel conformation coming from the experimental tubulin structure was assumed to be the bioactive one and used as a template model for all other taxanes. The EC paclitaxel conformation was transformed into a five-point pharmacophoric hypothesis by using the software Catalyst,[12] with the aim of finding the superimposition pathway of epothilones onto taxanes. We choose two hydrophobic features and three hydrogen bond acceptors as representative of the essential chemical functions of **1**. They corresponded to the phenyl ring bound to the C3' position, the C2 benzoyloxy group, the C1' carbonyl moiety, the C2' hydroxy group, and the oxetane oxygen, respectively.[5] The pharmacophoric model was then used as a three dimensional key to superpose epothilones onto paclitaxel by finding the common structural features shared by both compounds. In particular, the Best Fit option of Catalyst was applied to find, among all the conformers of each epothilone structure, the conformation able to satisfy the spatial constraints imposed by the pharmacophoric model. Two principal superimposition pathways were obtained, based on the orientation of the C15 side chain of epothilone B. In detail, *i.* in the first orientation, the C15 thiazole side chain of **16** was directed toward hydrophobic pocket 1 (HY1) of the pharmacophoric model, with hydrogen bond acceptor 1 (HBA1) and HBA2 mapped by the C1 carbonyl and C3 hydroxy groups, respectively. While the hydroxy moiety at the C7 position fitted the HBA3, HY3 was mapped by the C12 methyl substituent. *ii.* Alternately, in the second orientation, while the thiazole side chain matched HY2, the C1 carbonyl group overlayed HBA3. Moreover, the C5 carbonyl moiety and the C7 hydroxy substituent fitted HBA2 and HBA1, respectively. Finally, HY1 was reached by the C8 methyl group of epothilone B.

Next, the two proposed pharmacophoric models (to be intended as taxanes and epothilones superposed each other) were imported into the PrGen software[6] to perform the second step of our computational work. In detail, starting from the cocrystallized complex between paclitaxel and tubulin (1JFF PDB),[11] a shell of 15 Å around the ligand was selected and pruned according to mutagenesis and photoaffinity labeling studies. The resulting binding site of 32 amino acid residues (hereafter referred to as the minireceptor model) was then used to accommodate the two above described alignments of taxanes and epothilones, thus generating two different minireceptor-inhibitors assemblies, subsequently submitted to a calibration procedure. Particularly, a standard protocol consisting in an iterative equilibration and minimization of amino acid residues followed by minimization of inhibitors, was applied.

As a result, the minireceptor-ligands complex based on the first orientation of epothilones onto taxanes, gave encouraging statistical results and was worthy of a further optimisation. An original alignment hypothesis of all epothilones into taxanes was finally obtained (Fig. 3).

In particular, the oxetane oxygen atom corresponded to the hydroxy group at the 7-position of epothilone B, while the C1' carbonyl and C2' hydroxy substituents were matched by the C1 carbonyl group and C3 hydroxy group of epothilone, respectively. Finally, the C3' phenyl ring of **1** was superposed to the thiazole moiety of epothilone. The minireceptor with embedded the training set ligands (compounds **1**-**4**,**6**,**9**,**10**,**14**,**16**,**18**,**20**,**21**, Figure 1, Table 1) in the new original alignment, was optimized in PrGen using the same equilibration protocol described above in order to achieve optimum interaction pattern between the ligands and the residues. The 3D QSAR model obtained was able to correlate the structural properties of the training set compounds with their biological data, and was characterized by a correlation coefficient (R) of 0.81 and a root mean square deviation (rmsd) of 0.85 kcal/mol.

The overall fold of the newly generated pseudorecepor model and the orientation of taxanes within the binding site resembled the previous one. The binding pocket was principally represented by a hydrophobic environment with the macrocycle core structure of taxanes and epothilones retaining the optimal conformation to bring the substituents on the proper orientation to interact with the protein. In particular, the C4 acetyl, C12 methyl and C3' phenyl substituents lay in the same lipophilic region (mainly defined by Ala233, Ser236, and Phe272) locating the C3-C7 segment of epothilones. Moreover, the C3' benzamido and C2 benzoyl groups of taxanes lay in two different hydrophobic pockets, the latter defined by His229 and Leu 217, also accommodating the C12 substituent of epothilones (Fig. 4).

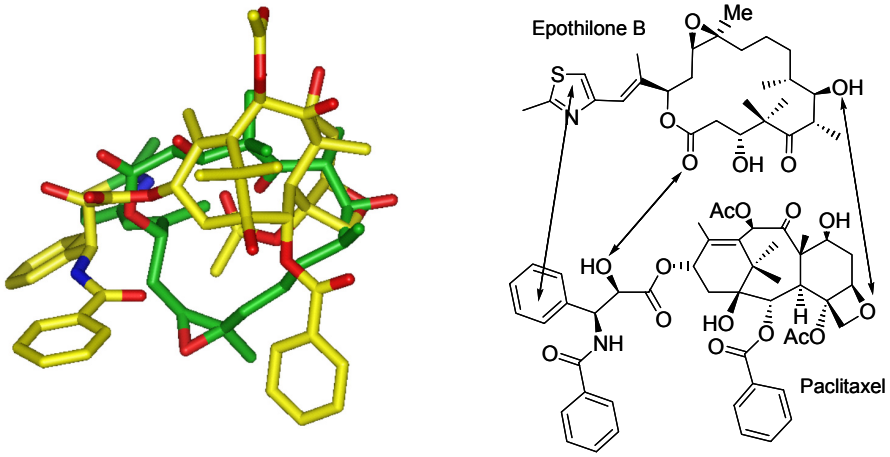

Figure 3. On the left, paclitaxel (1, yellow) superposed onto epothilone B (16, green), as resulting from minireceptor modeling approach. The C1 carbonyl group and C7 hydroxy moieties of 16 are superposed to the C2' hydroxy substituent and the oxetane ring of 1, respectively. Moreover, the thiazole side chain of 16 lies near the C3' phenyl ring of 1. The scheme on the right elucidates the common pharmacophore points of the two compounds.

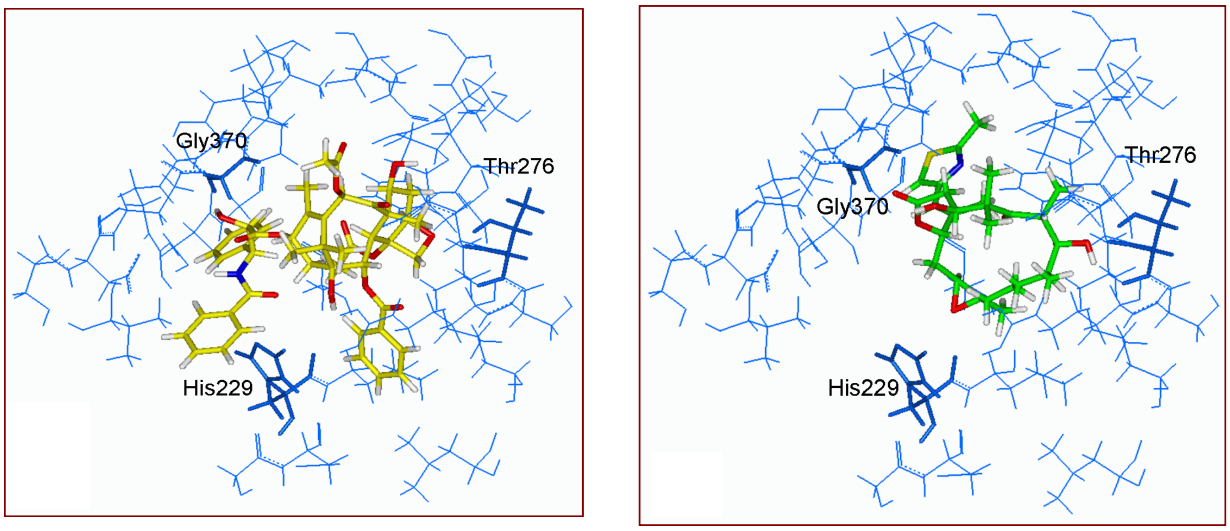

Figure 4. Paclitaxel (1, yellow, on the left) and Epothilone B (16, green, on the right) fitted into the minireceptor model (blue). A: The C2' hydroxy group and the oxetane ring of 1 are involved in hydrogen bonds with Gly 370 and Thr276, respectively. His229 is interposed between the C3' benzamido and C2 benzoyl moieties. B: Gly370 and Thr276 engage hydrogen bonds with the C1 carbonyl and C7 hydroxy groups of 16, respectively. Moreover, the C15 thiazole side chain is located in the same hydrophobic pocket also accommodating the C3' phenyl ring of 1.

Snyder and Downing have recently reported interesting results about the experimental binding mode of epothilone.[13] The authors suggest that tubulin displays a promiscuous binding pocket and that ligands like paclitaxel and epothilone exploits the tubulin-binding pocket in an independent manner. Accordingly, computational studies about the binding and pharmacophores for epothilones but also other microtubule-stabilizing agents as laulimalide, peloruside and colchicines,[14] will be further revised.

Nevertheless, due to the good quantitave structure-activity correlations obtained by our first optimised minireceptor model, we started to fit several taxanes into the model in order to find a new lead compound as anticancer drug. One of the most interesting taxanes fitted into our pseudoreceptor has been taxuspine U,[15] which seemed to adopt a paclitaxel-like bioactive conformation when docked into the binding pocket.

Taxuspine U (**22**) and X[16] (**23**) were found in methanolic extract of stems of genus *Taxus* and are constituted by the A ring of paclitaxel condensed with a 12-membered ring macrocycle (Figure 5). These two very rare bicyclic diterpenoids differ only for acetyl groups at C-2, C-7, C-20 and for a cinnamoyl group at C-5 position. The biological data of taxuspine U are not yet published but it is well known that taxuspine X is able to increase accumulation of vincristine in MDR cell lines, so it is interesting for overcoming multi-drug resistance.[17] Interestingly this compound is characterized by a cinnamoyl group at C-5, while lacking both an oxetane ring and a phenylisoserine group at C-13.

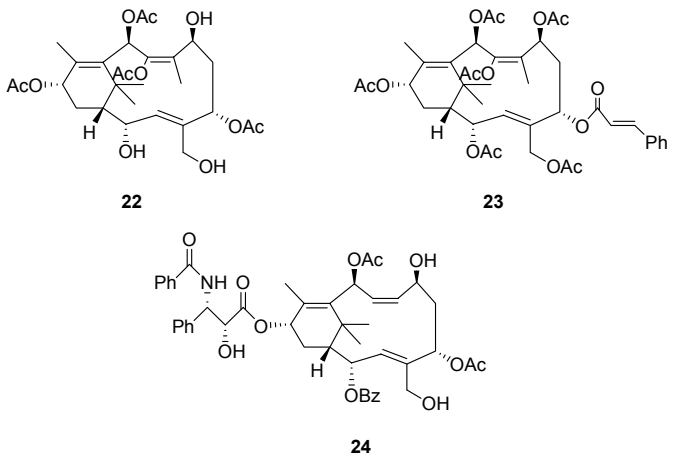

Figure 5

Once fitted into the tubulin binding site, the closely resemblance of taxuspine U 3D rearrangement to taxol bioactive conformation led us to design few structural modification of **22** (Figure 6, A), aimed at obtaining interesting molecule, such as **24** (Figure 5), potentially active as anticancer and/or MDR reversing agents. In particular, compound **24** (Figure 5 and 6) was designed through the following modifications:

- introduction of a benzoyl moiety, demonstrated to be one of the pharmacophoic feature of paclitaxel, on the C-2 OH;
- removal of substituents on Δ8 double bond, since they are not involved in any interaction with tubilin;
- protection or modification of the C-5 and C-10 OH groups, not engaged in interactions with the pseudoreceptor, in order to improve the bioavailability of the new compound;
- introduction of the C-13 β-phenylisoserine side chain of Taxol® on the C-13 position (Figure 6, B).

All the other moieties, providing interactions with the receptor or playing an important role in stabilizing conformations, are retained in molecule **24**, which was then aligned onto the conformation of paclitaxel and allowed to relax within the pseudoreceptor environment. The resulting conformation of **24** (Figure 6, C) shows a similar 3D shape with respect to that of paclitaxel and a similar orientation within the binding pocket. In particular, C-2 and C-13 side chains of **24** are engaged in hydrogen bonds with the protein, while C-7 and C-5 hydroxy groups are located far away from the pseudoreceptor residues and, consequently, they are not able to provide any profitable interaction. According to the modelled 5-minireceptor complex, only one hydrogen bond is missing with respect to Taxol® (Figure 7).

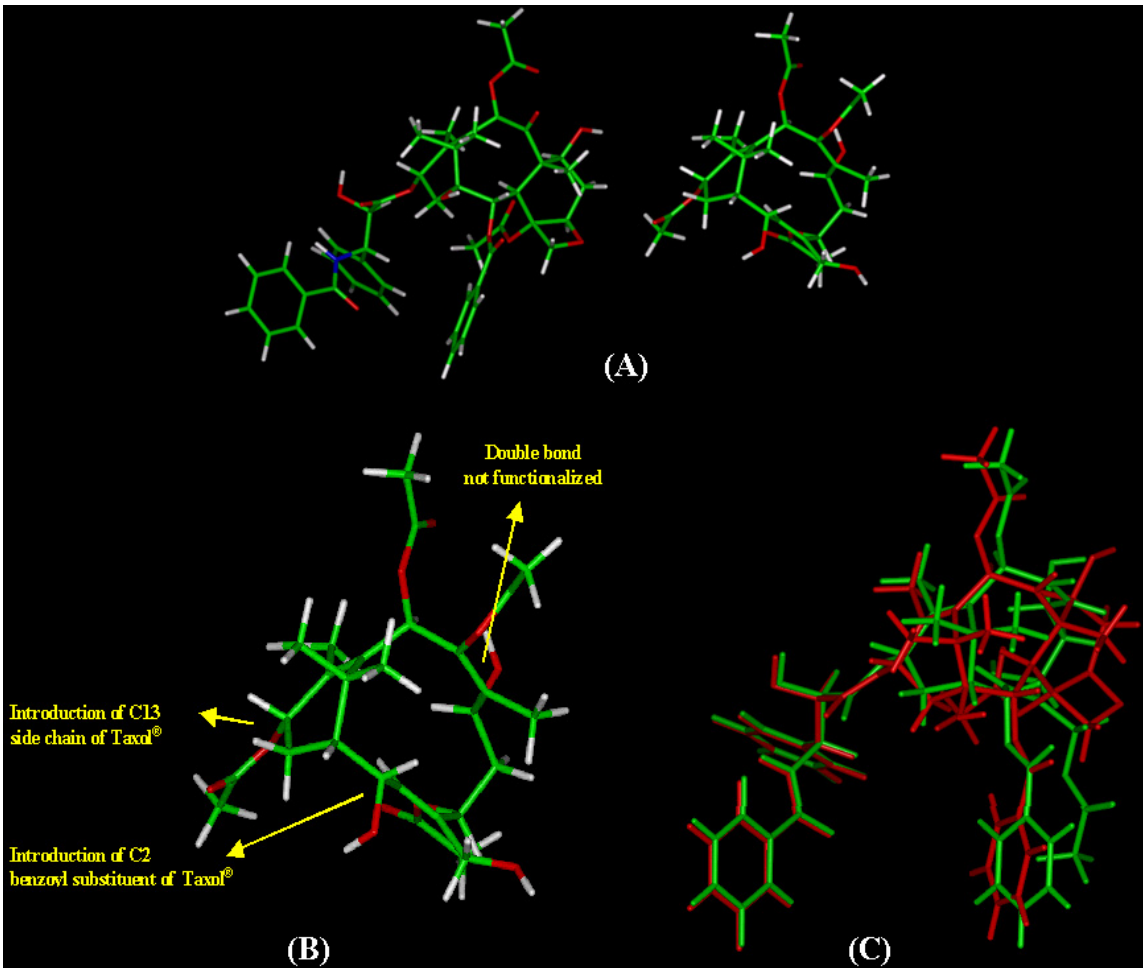

Figure 6. (A) 3D model of Taxol® (1, left) and Taxuspine U (3, right). (B) Structural modifications of natural Taxuspine U in order to achieve an anticancer drug. (C) Modified Taxuspine U with Taxol® side chain (24, green) superimposed to Taxol® (1, red).

Compound **24** (ΔG_{pred}=-6.429 Kcal/mol, Table 1) is predicted to be as active as Taxol® is (ΔG_{exp}=-6.464 Kcal/mol), while natural taxuspine U (**22**) is predicted by the model to be an extremely weak (ΔG_{exp}=-2.168 Kcal/mol) microtubules stabilizing agent. The similarity between the macrocycle conformation of **24**, and its orientation inside the binding site, suggested us that this class of compound might be a good candidate for replacing the pharmacophoric role of the ABC ring system of Taxol®, as outlined in Figure 7. Compound **24** is structurally simpler and synthetically more accessible than paclitaxel and could be an interesting alternative to the tricyclic taxanes, as an original lead compound for new microtubules stabilizing agents.

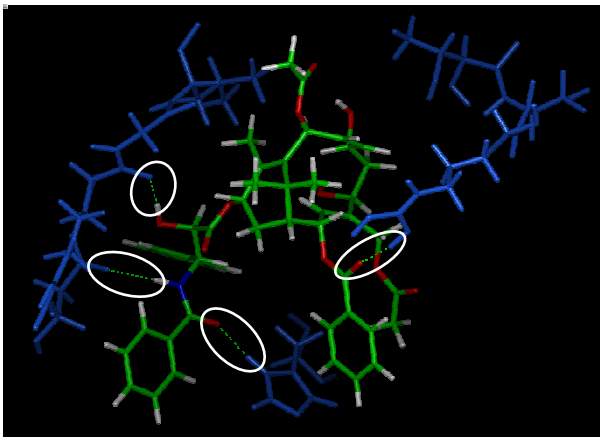

Figure 7. Taxuspine U-like compound 24 fitted into the minireceptor model. White circles highlight main ligand-protein interactions.

On the other hand, when a *trans*-cinnamoyl moiety is introduced on C-5 position and the β-phenyl isoserine side chain is removed, we are in presence of the Taxuspine X (**23**) analogue, that could be a lead compound for MDR reversing agents.

In this way, our project opens a pathway for the production of a variety of designed taxoids to be tested as anticancer and MDR reversing agents and represents a preliminary study for the synthesis of natural products taxuspine U and X.

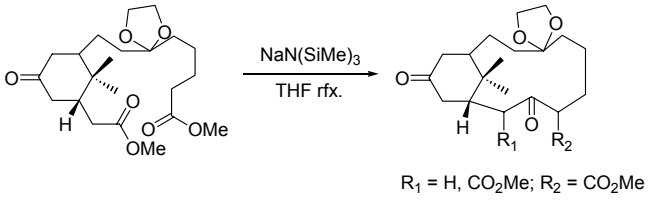

26 **27**

Scheme 1

Few years ago our research group described its own distinctive approach to the synthesis of a bicyclo[9.3.1]pentadecane skeleton **27** (Scheme 1), based on the Dieckman cyclization of a diester intermediate **26**.[18] The major shortcoming of that macrocyclization procedure, involving the not commercially available intermediate **26**, is the low reaction yield. Moreover, the macrocycle **27** thus obtained needs to be further functionalised for introducing the pharmacophoric moieties.

Accordingly, to obtain the target compound **24** we decided to apply different procedure than Dieckmann cyclization and we choose Ring Closing Metathesis (RCM) as the key step of our synthesis. RCM reaction is described to be reliable and seemed to us more versatile and compatible with the presence of diverse functional groups. This powerful and efficient reaction

involves α-ω dienes, and represents a unique carbon skeleton rearrangement in organic chemistry.[19]

Compounds **24** offers several points of disconnection and an interesting challenge for an original synthesis, since no many procedures for preparing this constrained 12 membered macrocycle have been reported in literature.[20] Moreover, the delivery of enantiomerically pure molecules was not our priority at the moment, as the biological data for these modified taxuspine-like compounds are yet not available.

Thus in the retrosynthetic analysis of **24**, after appropriate protections, removal of the Taxol®'s phenylisoserine side chain[21] and deoxygenation at the C-13 position[22] afforded a naked carbocyclic core (**25**), which was further simplified, leading to models **28** and **29**, more easily accessible for our preliminary studies *via* RCM-based macrocyclization reaction and useful to optimize the synthetic procedures, as outlined in Scheme 2.

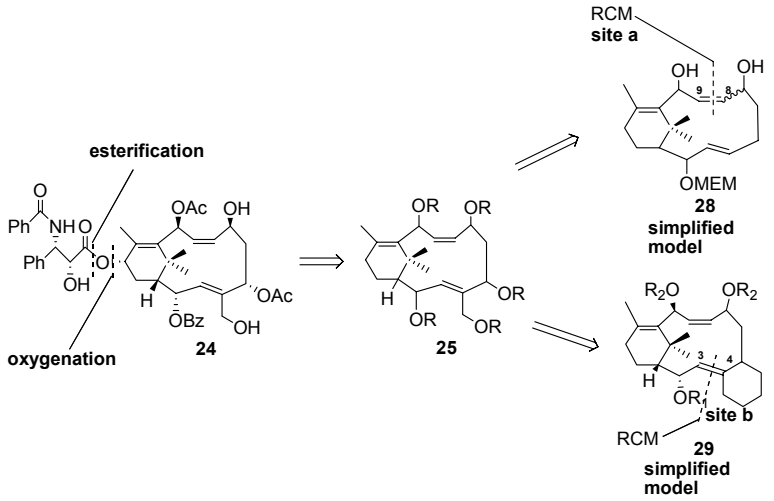

Scheme 2

In order to enhance the synthetic efficiency, two key points for the macrocyclization were initially considered in our retrosynthetic analysis of the target. Disconnection at *site a* afforded the first route in which the ω,ω'-diolefine intermediate was readly prepared as described in Scheme 3. Hydrozirconiation of **30** with the Schwartz reagent (Cp_2ZrHCl) gave the intermediate vinylzirconocene. Addition of aldehyde **31** and a catalytic amount of silver perchlorate ($AgClO_4$) resulted in the formation of the secondary alcohol **32**, as mixture of diastereoisomers, in 74% yield.[23] **32** was in turn protected on the secondary alcohol as methoxyethoxymethyl ether and the primary alcohols deprotected from the silyl ether and acetyl protecting group, obtaining **33**. Oxidation with Dess-Martin periodinane[24,25] provided the corresponding aldehyde which was converted into the terminal diolefine **28**.

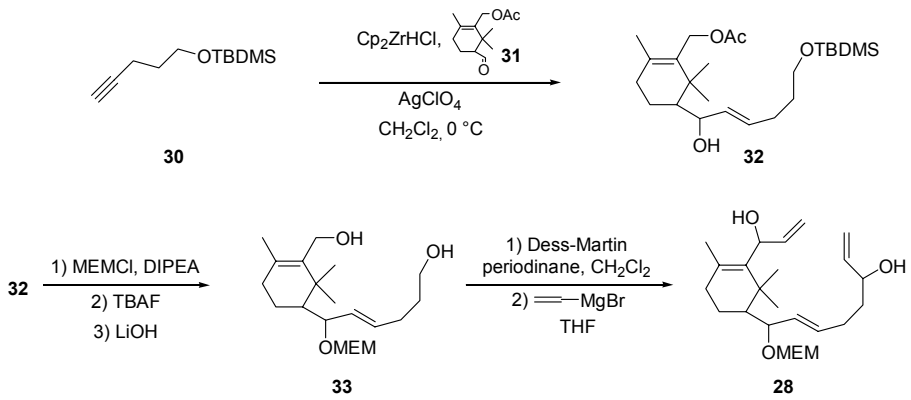

Scheme 3

28 was our first macrocycle precursor so it was treated with Grubbs catalyst in order to perform a macrocyclization *via* Ring Closing Metathesis.[26,27] Instead of the desired macrocycle, the methyl ketone **34** was formed (Scheme 4) through an unexpected reaction.

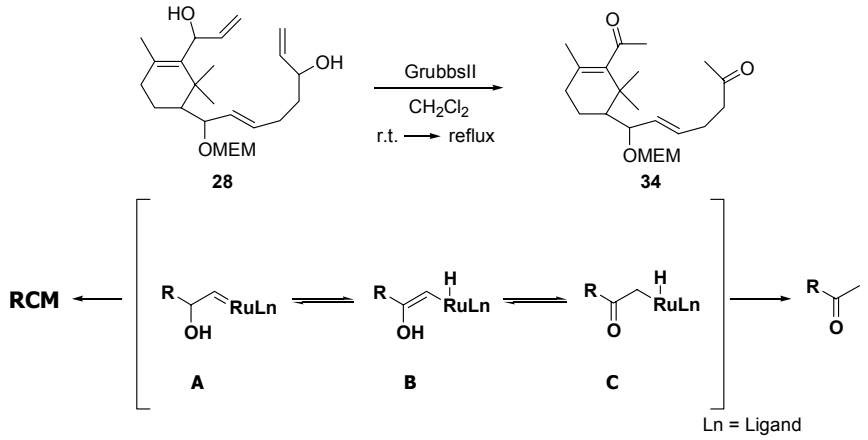

Scheme 4

It is clear that the ruthenium carbene species, coming from the Grubbs catalyst, was consumed by this side reaction, since use of only 10 mol % and 20 mol % of ruthenium catalyst results in low conversion of **28** and all the ^{1}H NMR resonances due to the catalyst disappear. It has been suggested[28,29] that the initial carbene A (Scheme 4) undergoes tautomerization to the enolyl ruthenium hydride species B, which can further undergo reductive elimination, either before or after tautomerization to the oxoalkyl ruthenium hydride C, to produce the methyl ketone.

In order to circumvent this side-reaction, **28** was subjected to oxidation with Dess-Martin periodinane, affording the ketone derivative **35**, which was treated with 20 mol % of Grubbs ruthenium catalyst in dry dichloromethane at room temperature and then at reflux (Scheme 5). Only traces (6%) of the desired macrocycle (**36**, Scheme 5) have been detected, together with:

compound **37**, resulting from the RCM between one double bond belonging to **35** and the benzylidene ligand of the catalyst as outlined in Scheme 6; compound **38**, resulting from the Ring Opening Metathesis at $\Delta^{3,4}$; five membered ring **39**, afforded by an intramolecular Ring Closing- Ring Opening Metathesis between the $\Delta^{3,4}$ and the terminal olefine, readily due to its relatively low strain (Scheme 6). In subsequent trials, we have also protected the allyl alcohols as silyl ether,[30] in order to make the alkene more electron-rich, and as acetyl ester, in order to reduce the sterical hindrance of the double bond, but in no case the desired macrocycle was detected.

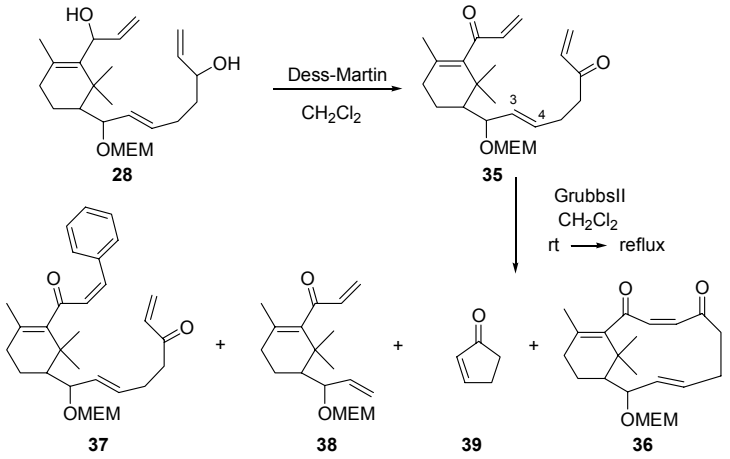

Scheme 5

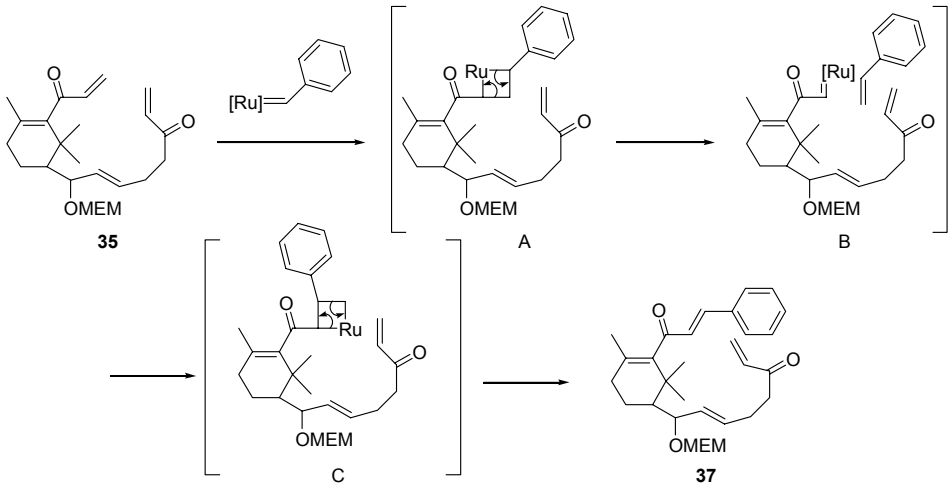

Scheme 6

As a consequence of these results, a second route was designed and the new ω-ω'- diolefine intermediate **29** (Scheme 2) was envisioned to be the macrocycle precursor for the RCM.

More in detail (Scheme 7), in a retrosynthetic sense, the disconnection of the B-ring of **29** between C_3-C_4 at the *site b* leads to **40**, which is an ω-ω' di-olefine intermediate and can be cyclized by RCM to the desired macrocycle, while the *cis*-$\Delta^{8,9}$ double bond is expected to result from selective reduction of the corresponding triple bond. The second bond disconnection was planned between C_7-C_8 furnishing a highly convergent approach to the taxane nucleus from a suitably functionalized ring A building block **41** and aldehyde **42**.

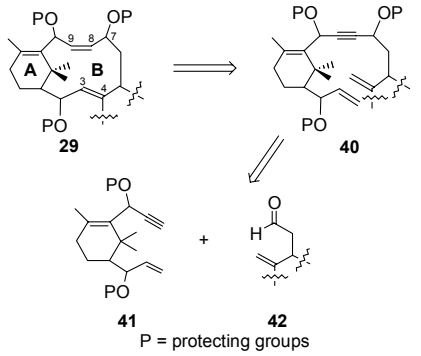

Scheme 7

The first intermediate we examined was **41**, which incorporate the alkyne functionality, built for the coupling with an aldehyde, and the alkene functionality necessary for the metathesis macrocyclization.

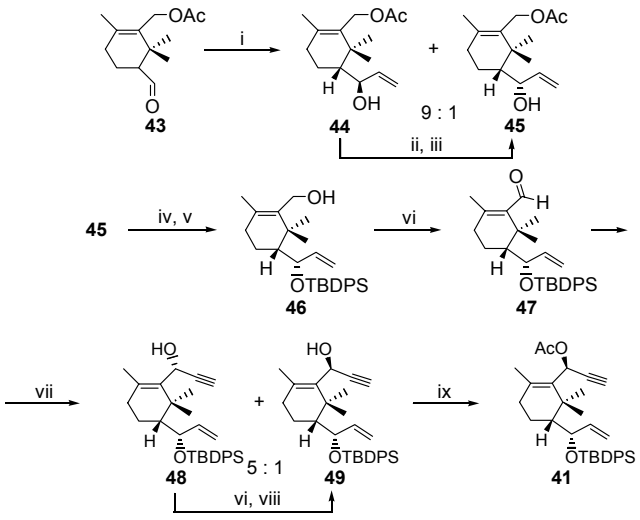

Scheme 8. Reagents, conditions and yields: (i) vinylmagnesium bromide, THF -78°C to r. t., 84%; (ii) Dess Martin periodinane, CH_2Cl_2, 90%; (iii) L-Selectride, THF -78°C to r.t., 84%; (iv) TBDPSCl, imidazole, DMAP, DMF r. t., 85%; (v) K_2CO_3, CH_3OH, quantitative; (vi) TPAP, MNO, mol. siev., CH_2Cl_2, r. t., 91%; (vii) ethynylmagnesium bromide, THF -78°C to r. t., 85%; (viii) 9-BBN, THF, 0°C, 90%; (ix) Ac_2O, Et_3N, DMAP, CH_2Cl_2, r. t., quantitative.

The alkyne **41** was obtained according to Scheme 8. Treatment of the known aldehyde **43**[31] with a small excess of a vinylmagnesium bromide, at low temperature, led to a mixture of **44** and **45** with high level of diastereoselectivity (9:1, with an excess of the **44** *syn* compound), resulting from the preferential attack opposite to the *gem* dimethyl group in which the carbonyl group is also oriented away from these substituents.[32] The most abundant isomer **44** was converted into **45** by oxidation with Dess-Martin periodinane followed by reduction to alcohol of the ketone derivative with L-Selectride.[33] The ortogonal protection of the allyl alcohol **45** as TBDP silyl ether derivative, followed by a basic hydrolysis of the O-acetyl group, produced the corresponding alcohol derivative **46**, which on oxidation with TPAP-MNO[34] was then converted into the aldehyde **47** in 95% yield. When the aldehyde **47** was reacted with ethynylmagnesium bromide, a mixture of two diastereoisomers **48** and **49** was obtained in a ratio of 5:1. This stereochemical result arose from the preferred approach from the top of the molecule with the cabonyl group oriented downward in order to minimize the interaction with the adjacent methyl groups.[35] The resulting propargyl alcohols **48** and **49** were separated by flash chromatography and **48** converted into the most interesting diastereoisomer **49** by oxidation of the alcohol to ketone with TPAP-MNO, followed by reduction with 9-BBN.[36] The propargyl alcohol **49** was finally acetylated to provide the intermediate **41**.

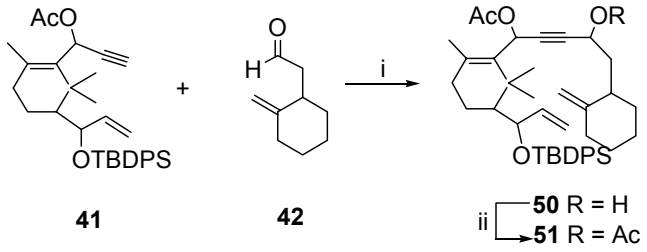

Scheme 9. Reagents, conditions and yields: (i) LHMDS, THF -78 °C to r. t., 65-72%; (ii) Ac_2O, Et_3N, DMAP, CH_2Cl_2, r. t., quantitative.

As outlined in Scheme 9, the macrocycle precursors **51** was prepared by reaction of the lithiated derivative of **41** with aldehydes **42** in THF at –78 °C. Subsequent acetylation in classical condition of the newly formed alcohol provided **51**.

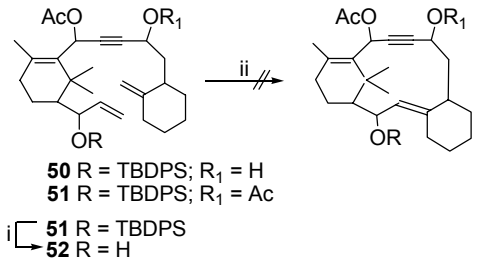

Scheme 10. Reagents, conditions and yields: (i) TBAF, THF, 40 °C, 62%; (ii) Grubbs I and II ruthenium catalyst, Schrock's catalyst, CH_2Cl_2 or toluene.

The relative stereochemistry of the newly formed chiral center was not our priority at that stage of our work, as previously pointed out, and with this original macrocycle precursor in our hands, we went on to study the key reaction of our sequence. Different RCM assays were performed on the ω-ω' di-olefine intermediates **50** and **51** but in no case intramolecular cyclization occurred and the starting material was consistently recovered, either varying the RCM conditions and the metathesis catalysts used (Grubbs I, Grubbs II ruthenium catalyst or Schrock's catalyst). In order to reduce the sterical hindrance of the double bond and help the complexation between the catalyst and the substrates, the silyl ether in the allyl position was cleaved, giving the corresponding alcohol **52**, but also with these less hindered substrates the macrocyclization failed, giving the unaltered starting material (Scheme 10).

Attempts to rationalize these results using computer modeling and energy minimizations data in order to verify the statistical possibility to find conformers with the ω-ω' double bond at an appropriate distance for giving a new double bond,[37] were not helpful, suggesting that the best precursors of the macrocycle were **50**, **51** and **52**. In any case, the problem of the RCM was clearly not correlated to the sterical hindrance of the double bonds involved in the reaction. We reasoned that the alkyne function present in the precursors previously described could affect the catalyst so as to wreck our plan of RCM. Aside from the constraint to cyclization imposed by the linear character of the acetylene group, the cyclization could further be complicated by non productive coordination of the triple bond to the RCM catalytic machinery.[38] To the best of our knowledge, in fact, no other example of olefine metathesis is described involving molecules bearing also a triple bond.

Conversely, the partial hydrogenation of **51** to the corresponding *cis*-alkene with Lindlar catalyst and quinoline proved to be effective and we obtained the new macrocycle precursor **53** in high yield. Finally RCM using 10% Grubbs II catalyst on the ω,ω'-diolefine **53** gave in 20% yield the desired macrocycle **55**,[39] a 3,8 secotaxane diterpenoid, simplified analogue of taxuspine U, which is the first target of this work (Scheme 11). Similar result was obtained in the macrocyclization of **54**, the fully deprotected derivative of **53**.

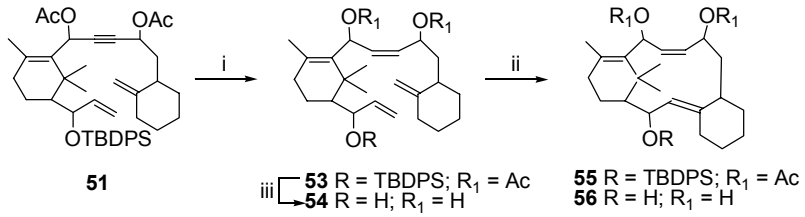

Scheme 11. Reagents, conditions and yields: (i)H2, Lindlar catalyst, quinoline, petrol ether, 90%; (ii) Grubbs II ruthenium catalyst, CH_2Cl_2, 20 and 25%; (iii) a:TBAF, THF, 40°C, 75%; b: K_2CO_3, CH_3OH, quantitative.

In conclusion, we have developed an elegant and new methodology for the synthesis of simplified taxuspines U analogues. This methodology involves a macrocyclisation reaction of a

12 membered strained ring *via* RCM in presence of different functional groups. The different RCM assays done on the macrocycle precursor have shown the negative influence of the akyne function, as already reported also by Danishefsky and coworkers.[38] Finally, this synthesis pathway is a part of a wider project aimed at the design and synthesis of new microtubules stabilizing antimitotic agents and MDR-reversing agents. The identification of microtubule stabilizing agents as promising anticancer drugs has spurred a lot of studies about their synthesis, biological evaluation, pharmacophore generation and investigation on the interactions with tubulin. Since the discovery of paclitaxel's unique mechanism of action, more than two decades have elapsed, and the MSAAs family includes today taxanes, epothilones, sarcodictyins, eleutherobins, and discodermolide. Moreover a similar mechanism of action has been proposed also for other analogs including laulimalide, WS9885B, some polyisoprenyl benzophenones and even steroid derivatives. While many new analogs are isolated or synthesized and tested, it is also known that a productive rational drug design may only be achieved with the knowledge of the molecular interactions between the ligands and the protein. The EC structure of tubulin with embedded paclitaxel has been a great help to gain insight into this question and only similar experimental studies for each of the above mentioned classes of compounds will elucidate the problem of defining the bioactive conformation of ligands within the protein and consequently the essential pharmacophore points responsible for antimitotic activity. In this context, the minireceptor approach is a useful tool that allows to develop 3D QSAR models comprehensive of the protein environment. With the aim of optimizing a previous minireceptor model for taxanes only, a second model was developed starting from both the refined EC structure of tubulin and an original pharmacophore model for taxanes and epothilones. Agreement with SAR and experimental data reported in literature validate the model and make it a consistent tool to address the design of new compounds.

Acknowledgments

We are grateful to the Research Training Network (HPRN-CT-2000-00018) “Design and Synthesis of Novel Paclitaxel (Taxol®) Mimics Using a Common Pharmacophore Model for Microtubule-Stabilizing Agents (MSAAs)”, FIRB (RBAU01LR5P) “Development of a Common Pharmacophore Model for Microtubule-Stabilizing Anticancer Agents to be used to Design and Synthesise Novel Paclitaxel Mimics” for the financial support. One of us (M.B.) thanks the MerckResearch Laboratories for the 2002 Academic Development Program (ADP) Chemistry Award and Dr. Paolo Malizia for a support at the beginning of his career.

References

1. Wani, M. C.; Taylor, H. L.; Wall, M. E.; Coggon, P.; McPhail, A. T. *J. Am. Chem. Soc.* **1971**, *93*, 2325.

2. MacDonald, T.; Landino, L. In *TAXOL: Science and Applications*; Suffness, M. Ed.; CRC Press: Boca Raton, FL, 1995; pp301-335.
3. Horwitz, S. B. *Trends Pharmacol. Sci.* **1992**, *13*, 134.
4. (a) Snyder, J. P.; Nettles, J. H.; Cornett, B.; Downing, K. H.; Nogales, E. *Proc. Natl. Acad. Sci. USA* **2001**, *98*, 5312. (b) Wang, M.; Xia, X.; Kim, Y.; Hwang, D.; Jansen, J. M.; Botta, M.; Liotta, D. C.; Snyder, J. P. *Org. Lett.* **1999**, *1*, 43.
5. (a) Maccari, L.; Manetti, F.; Corelli, F.; Botta, M. *Il Farmaco* **2003**, *58*, 659. (b) Manetti, F.; Maccari, L.; Corelli, F.; Botta, M. *Curr. Top. Med. Chem.*, **2004**, *4*, 203.
6. Zbinden, P. PrGen 2.1.1 Biographics Laboratory, Basel, Switzerland.
7. Nogales, E.; Wolf, S.G.; Downing, K.H. *Nature* **1998**, *391*, 199.
8. Gueritte-Voegelein, F.; Guenard, D.; Mangatal, L.; Potier, P.; Guilhem, J.; Cesario, M. *Acta Crystallogr. C* **1990**, *46*, 781.
9. (a) Snyder, J. P.; Nettles, J. H.; Cornett, B.; Downing, K. H.; Nogales, E.. *Proc. Natl. Acad. Sci. USA* **2001**, *98*, 5312. (b) Milanesio, M.; Ugliengo, P.; Viterbo, D.; Appendino, G.. *J. Med. Chem*. **1999**, *42*, 291. (c) Snyder, J. P.; Nevins, N.; Cicero, D. O.; Jansen, J. J. *J. Am. Chem. Soc*. **2000**,*122*, 724.
10. Manetti, F.; Forli, S.; Maccari, L.; Corelli, F.; Botta, M. *Il Farmaco* **2003**, *58*, 257.
11. Lowe, J.; Li, H.; Downing, K. H.; Nogales, E. *J. Mol. Biol.* **2001**, *313*, 1045.
12. *Catalyst*, version 4.6: Accelrys, Inc., 9685 Scranton Road, San Diego, CA.
13. Nettles, J. H.; Li, H.; Cornett, B.; Krahn, J. M.; Snyder, J. P.; Downing, K. H. *Science* **2004**, *305*, 856.
14. Pineda, O.; Farràs, J.; Maccari, L.; Manetti, F.; Botta, M.; Vilarrasa, J. *Biorg. Med. Chem. Lett.* **2004**, *14*, 4825.
15. Hosoyama, H.; Inubushi, A.; Katsui, T.; Shigemori, H.; Kobayashi, J. *Tetrahedron* **1996**, *52*, 13145.
16. Shigemori, H.; Wang, X-X.; Yoshida, N.; Kobayashi, J. *Chem. Pharm. Bull.* **1997**, *45*, 1205.
17. Kobayashi, J.; Shigemori, H. *Med. Res. Rev.* **2002**, *22*, 305.
18. Corelli, F.; Dei, D.; Menichincheri, M.; Snyder, J. P.; Botta, M. *Tetrahedron Lett.* **1997**, *38*, 2759.
19. Grubbs, R. H.; Pine, S. H. In *Coomprehensive Organic Synthesis*; V. 5, Trost, B. M., Fleming, I., Eds.; Pergamon Press: Oxford, England, 1991; pp 1115-1127.
20. Renzulli, M.; Rocheblave, L.; Avramova, S.; Corelli, F.; Botta, M. *Tetrahedron Lett.* **2004**, *45*, 5155 *and references therein cited*.
21. Castagnolo, D.; Armaroli, S.; Corelli, F.; Botta, M. *Tetrahedron: Asymmetry* **2004**, *15*, 941.
22. Nicolaou, K. C.; Nantermet, P. G.; Ueno, H.; Guy, R. K.; Couladouros, E. A.; Sorensen, E. J. *J. Am. Chem. Soc.* **1995**, *117*, 624 *and references therein cited*
23. Richter, F.; Bauer, M.; Perez, C.; Maiale-Mössmer, C.; Maier, M. E. *J. Org. Chem.* **2002**, *67*, 2474 *and references therein cited*.
24. Dess, D. B.; Martin, J. C. *J. Am. Chem. Soc.* **1991**, *113*, 7277.
25. Meyer, S. D.; Schreiber, S. L. *J. Org. Chem.* **1994**, *59*, 7549.

26. Fu, G. C; Grubbs, R. H. *J. Am. Chem. Soc.* **1992**, *114*, 5426.
27. Schrock, R. R.; Murdzek, J. S.; Bazan, G. C.; Robbins, J.; DiMare, M.; O'Regan, M. *J. Am. Chem. Soc.* **1990**, *112*, 3875.
28. Hoye, T. R.; Zhao, H. *Org. Lett.* **1999**, *1*, 169.
29. Hoye, T. R.; Zhao, H. *Org. Lett.* **1999**, *1*, 1123.
30. Corey, E. J.; Venkateswarlu, A. *J. Am. Chem. Soc.* **1972**, *94*, 6190.
31. Hitchcock, S.A.; Houldsworth, S.J.; Pattenden, G.; Pryde, D.C.; Thomson, N.M.; Blake, A.J. *J.Chem.Soc.Perkin Trans.1* **1998**, *19*, 3181.
32. Tjepkema, M. W.; Wilson, P. D.; Audrain, H.; Fallis, A. G. *Can. J. Chem.* **1997**, *75*, 1215.
33. Winkler, J. D.; Bhattacharya, S. K.; Batey, R. A. *Tetrahedron Lett.* **1996**, *37*, 8069.
34. Ley, S.V.; Norman, J.; Griffith, W.P.; Marsden, S.P. *Synthesis* **1994**, *7*, 639.
35. Tjepkema, M. W.; Wong, T.; Wilson, P. D.; Fallis, A. G. *Can. J. Chem.* **1997**, *75*, 1542.
36. Krishnamurthy, S.; Brown, H. C. *J. Org. Chem.* **1977**, *42*, 1197.
37. Bernardini C. Master Thesis, University of Sienna, 2002.
38. Yang, Z.-Q.; Geng, X.; Solit, D.; Pratilas, C. A.; Rosen, N.; Danishefsky, S. J. *J. Am. Chem. Soc.* **2004**, *126*, 7881.
39. **55.** IR (film): ν 3080, 1740, 1660, 979 cm^{-1}. ^1H NMR (200 MHz, $CDCl_3$) δ 7.69-7.61 (m, 5H), 7.40-7.28 (m, 5H), 6.32 (d J = 5 Hz, 1H), 5.74 (dd *J* = 5, 7 Hz, 1H), 5.55 (dd *J* = 6, 7 Hz, 1H), 5.4 (m, 1H), 5.1 (d *J* = 10 Hz, 1H), 4.32 (dd *J* = 2.5, 10 Hz, 1H), 2.35-2.18 (m, 4H), 2.06 (s, 3H), 2.02 (s, 3H), 1.97-1.87 (m, 3H), 1.85 (s, 3H), 1.70-1.65 (m, 5H), 1.30-1.20 (m, 4H), 1.1 (s, 3H), 1.02 (s, 9H), 0.97 (s, 3H). ESI-MS (*m/z*): 707 $[M+K]^+$, 691 $[M+Na]^+$, 668 $[M+H]^+$. Anal. Calcd for $C_{42}H_{56}O_5Si$: C, 75.41; H, 8.44; O, 11.96. Found: C, 75.15; H, 8.76; O, 12.11.
56. IR (film): ν 3440, 3080, 1660, 979 cm^{-1}. ^1H NMR (200 MHz, $CDCl_3$) δ 5.6 (dd J = 5, 7 Hz, 1H), 5.5 (d, *J* = 6 Hz, 1H), 5.45 (dd, *J* = 7, 7.5 Hz, 1H), 5.15 (d, *J* = 10 Hz, 1H), 4.45 (br d, *J* = 10 Hz, 1H), 4.38 (dd, *J* = 6, 7.5 Hz, 1H), 2.35-2.18 (m, 5H), 1.97-1.87 (m, 3H), 1.85 (s, 3H), 1.70-1.65 (m, 6H), 1.30-1.20 (m, 5H), 1.1 (s, 3H), 0.97 (s, 3H). ESI-MS (*m/z*): 385 $[M+K]^+$, 369 $[M+Na]^+$, 347 $[M+H]^+$. Anal. Calcd for $C_{22}H_{34}O_3$: C, 76.26; H, 9.89; O, 13.85. Found: C, 75.81; H, 10.54; O, 13.65.